Observing the Importance of the Phase-Volume Effect for Few-Cycle Light-Matter Interactions

Yinyu Zhang,[1] Danilo Zille, Dominik Hoff, Philipp Wustelt, Daniel Würzler, Max Möller, A. M. Sayler, and Gerhard G. Paulus

Institute of Optics and Quantum Electronics, Friedrich Schiller University Jena, Max-Wien-Platz 1, 07743 Jena, Germany and Helmholtz Institute Jena, Fröbelstieg 3, 07743 Jena, Germany

(Received 10 December 2019; revised manuscript received 25 February 2020; accepted 10 March 2020; published 31 March 2020)

The spatially dependent phase distribution of focused few-cycle pulses, i.e., the focal phase, is much more complex than the well-known Gouy phase of monochromatic beams. As the focal phase is imprinted on the carrier-envelope phase (CEP), for accurate modeling and interpretation of CEP-dependent few-cycle laser-matter interactions, both the coupled spatially dependent phase and intensity distributions must be taken into account. In this Letter, we demonstrate the significance of the focal phase effect via comparison of measurements and simulations of CEP-dependent photoelectron spectra. Moreover, we demonstrate the impact of this effect on few-cycle light-matter interactions as a function of their nonlinear intensity dependence to answer the general question: if, when, and how much should one be concerned about the focal phase?

DOI: 10.1103/PhysRevLett.124.133202

The rapid development of technologies for the generation of intense few-cycle laser pulses from the extreme ultraviolet to midinfrared [1–9], has allowed for the investigation of an ever-broadening range of light-matter interactions in the few-cycle regime. One particular interest is the ability to sculpt the wave form of few-cycle pulses via the phase of the carrier wave with respect to the envelope, the so-called carrier-envelope phase (CEP). As the laser-induced dynamics depends on the electric field, control of the CEP directly results in a broad range of applications, such as isolated attosecond pulse generation [10–12], selection of high-harmonic generation peaks [13–15], control of THz-emission [16,17], study of electron dynamics in atomic [18–21], molecular [22–25], and solid state [26] systems.

An important effect, which is often neglected in the analysis of these phenomena, is the spatial dependence of the CEP of a focused beam. Even when it is included, the usual assumption for this dependence is the well-known Gouy phase, $\Delta\Phi_G = -\arctan(z/z_R)$ [27], where z is the beam propagation position and z_R is the Rayleigh length. This spatially dependent phase distribution in the laser focus shown in Fig. 1(b), is coupled to the cycle-averaged intensity distribution, shown in Fig. 1(a). Thus, the target, e.g., atoms or molecules inside the focus experience different laser intensities and CEPs depending on their positions. The intensity distribution leads to an averaging effect on intensity-dependent phenomena, the so-called intensity-volume effect [28]. Similarly, for phenomena induced by few-cycle pulses, the CEP dependence will be partially averaged out due to the phase distribution, which we refer to as the "phase-volume effect." In other words, theoretical modelling that does not take into account the phase distribution, will predict a stronger phase dependence than actually measured.

The aforementioned Gouy phase is derived for monochromatic beams. However, the majority of CEP-dependent effects become observable only when the pulse duration consists of a few optical cycles, which requires a broad frequency bandwidth. Therefore, considering only the monochromatic phase shift is insufficient. The frequency-dependent Gouy phase and its effect started to draw researchers attention [30–32]. Based on diffraction theory, M. A. Porras derived a more general description of the phase shift for broadband pulses [33–35], which we refer to here as the focal phase:

$$\Delta\Phi_F(r,z) = -\arctan\left(\frac{z}{z_R}\right) + \frac{g_0[1-2(\frac{r}{w(z)})^2]}{\frac{z}{z_R}+\frac{z_R}{z}}, \quad (1)$$

with

$$g_0 = \left.\frac{dZ_R(\omega)}{d\omega}\right|_{\omega_0} \frac{\omega_0}{Z_R(\omega_0)}, \quad (2)$$

$$Z_R(\omega) = \omega W(\omega)^2/2c, \quad (3)$$

where r is the radial position, ω_0 is the center frequency of the laser, $w(z)$ is the z-dependent beam radius of the center frequency, $Z_R(\omega)$ is the frequency-dependent Rayleigh range of the collimated input beam, $W(\omega)$ is the frequency-dependent input waist, and c is the speed of light. The focal waist is at the position $z = 0$. In this formulation,

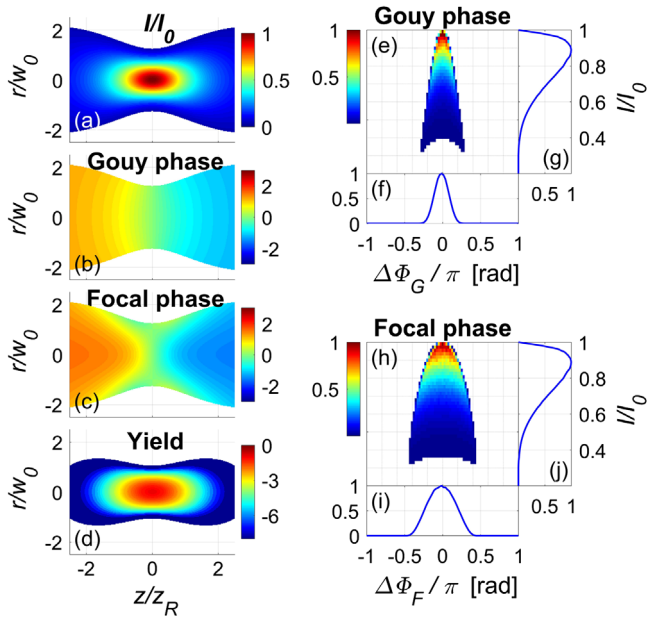

FIG. 1. (a) Intensity distribution of a focused Gaussian laser beam (linear scale). I_0 is the peak intensity, w_0 is the beam waist and z_R is the Rayleigh range at center frequency. (b),(c) The spatial distribution of the Gouy phase and the focal phase with a Porras factor $g_0 = -2$. (d) The intensity-dependent ionization yield in log-scale estimated by the ADK rate [29]. (e),(h) The normalized phase- and intensity-dependent yield of the Gouy phase and the focal phase. (f),(i) The projection of the yield on the phase axis and (g),(j) on the intensity axis, respectively.

an extra term modifying both the on-axis phase and radially dependent phase is added to the familiar Gouy phase, see Eq. (1). The Porras factor, g_0, describes the frequency-dependent spectral diameter and the spectral divergence of the input beam, see Eq. (2). Characteristic examples are input beams with (i) $g_0 = 0$, which reverts back the monochromatic approximation (Gouy phase), (ii) $g_0 = -1$, which has a frequency-independent divergence, and (iii) $g_0 = 1$, which has a frequency-independent waist. Additional deviations from this formulation may become important to account for higher order effects or poor beam quality. However, we find that this formulation without additional higher-order corrections is sufficient to accurately reproduce the measured phase distribution.

Here, we will focus primarily on the situation where $g_0 < -1$ for two reasons. First, this corresponds to the typical geometry of few-cycle pulse generation systems based on the hollow-core fiber-compressor (HFC). Namely, the diameter of frequency components are confined by the exit of the fiber and long wavelengths have large divergence propagating in free space. Thus, after the collimation of the beam, the long wavelength (red) radius is larger than the short wavelength (blue) radius, resulting in a larger Rayleigh range, $Z_R(\omega)$, which corresponds to the situation where $g_0 < -1$. Second, a Porras factor of -2.1 ± 0.2 was directly measured [36] for such geometry. Therefore, for typical HFC-based laser systems, $g_0 = -2$ is a good assumption. However, if one has a laser system not conforming to this geometry, the Porras factor must be measured to determine the exact phase distribution. The focal phase distribution with $g_0 = -2$, shown in Fig. 1(c), shows significantly larger phase shifts than the Gouy phase, shown in Fig. 1(b). As a consequence, the phase-volume effect due to the phase distribution of few-cycle pulses is significantly stronger than generally assumed for the monochromatic case.

In this Letter, we demonstrate the importance of the phase-volume effect, i.e., the reduction of the CEP-dependence due to averaging the CEP in the focus. First, we compare measurements and simulations of the asymmetry obtained from the CEP-dependent photoelectron emission in opposing directions in xenon at different laser wavelengths to illustrate and quantify the phase-volume effect in different experimental configurations. Further, building upon this knowledge, we formulate a more general description of the impact of the focal phase for laser-matter interactions with different nonlinear intensity dependencies to answer the general question: if, when, and how much should one be concerned about the phase-volume effect?

First, we illustrate the quantitative differences between the Gouy phase and the focal phase to demonstrate the significance of the phase-volume effect of few-cycle pulses. For a Gaussian laser beam, the intensity distribution near the focus is shown in Fig. 1(a). The spatial distribution of the Gouy phase is shown in Fig. 1(b). In contrast, a more realistic case of few-cycle pulses, with $g_0 = -2$, has a very different phase distribution, see Fig. 1(c). Combining the phase distribution and the intensity-dependent yield of a certain physical process, an intensity- and phase-dependent yield can be calculated. Here, we select strong-field ionization as a characteristic instance and quantify the phase-volume effect for this process as a baseline. Assuming that (i) the target, i.e., atoms or molecules, has a uniform density and (ii) the probability of strong-field ionization at different intensities can be estimated applying the commonly used Ammosov-Delone-Krainov (ADK) ionization rate [29], the phase-averaged intensity-dependent yield for strong-field ionization is obtained, see Fig. 1(d). The phase- and intensity-dependent yield can be obtained [Figs. 1(e) and 1(h)] by calculating a two-dimensional histogram of the spatially-dependent phase and the intensity weighted by the yield (details see the Supplemental Material [37]).

The projection of this yield on each axis illustrates the intensity-volume and the phase-volume effects individually. The intensity-dependent yield, shown in Figs. 1(g) and 1(j), demonstrate the intensity-volume effect, which implies two important consequences: (i) the maximum of the intensity-dependent probability appears at an intensity well below the peak intensity, I_0. This is because the increasing probabilities at higher intensities approaching I_0 cannot counteract the vanishingly small interaction volume.

(ii) Instead of a single intensity dependence, all intensities below the peak intensity make various contributions. Here, the mean value is $\sim 0.80 I_0$ and the rms of the distribution is $\sim 0.13 I_0$.

Similarly, the projection of the yield on the phase-axis illustrates the phase-volume effect, which results in averaging of the CEP and a reduction of the strength of CEP effects, see Figs. 1(f) and 1(i). If the phase is not taken into account, the phase distribution in Figs. 1(f) and 1(i) will be a Dirac delta function at zero. For a monochromatic beam, the rms of the phase distribution is $\sim 0.09\pi$ rad. In contrast, for broadband pulses, the rms of the phase distribution increases significantly and varies from 0.20π to 0.27π rad, with a g_0 factor in a range from -1.5 to -2.5, which corresponds to achievable frequency-dependent beam radius for typical fiber-compressor based few-cycle laser systems. For the $g_0 = -2$ case detailed here, the corresponding rms is $\sim 0.25\pi$ rad. Comparing to the Gouy phase case, the roughly factor of 3 times wider phase distribution implies a much stronger averaging effect and leads to a more significantly smearing out of any measured CEP dependence.

In order to show this focal phase effect concretely, let us examine the strong-field ionization of xenon. We use ~12-fs, 1800-nm pulses to ionize xenon atoms around the barrier-suppression intensity (0.8×10^{14} W/cm^2). The CEP-dependent photoelectron spectra, also called above-threshold ionization (ATI) spectra [18,38,39], are measured by a high-resolution time-of-flight (TOF) spectrometer. The spatial asymmetry A is obtained by analyzing the normalized difference between the photoelectron spectrum emitting to opposing directions along the laser polarization axis: $A = (S_l - S_r)/(S_l + S_r)$, where S_l and S_r indicate the spectra measured at two directions. The measured asymmetry probed with ~12-fs, 1800-nm pulses is shown in Fig. 2(a).

A standard one-dimensional time-dependent Schrödinger equation (TDSE) simulation is applied to calculate the left-right asymmetry and compared to the measurements. The simulated asymmetry using a single intensity considering neither the intensity-volume nor the phase-volume effect are shown in Fig. 2(b). Comparing this with the simulated asymmetry considering only the intensity-volume effect and not the phase-volume effect [see Fig. 2(c)], and with simulations including both effects [see Fig. 2(d)], one can clearly see the blurring of phase dependence due to the intensity- and phase-volume effect. The strength of the asymmetry for each energy region becomes smaller when the focal phase is included in the simulation, producing a better agreement with the measurements.

To quantify the phase-volume effect in strong-field ionization directly, we look at the carrier-envelope phase-meter (CEPM) traces at 1800 nm laser wavelengths, which are based on the measurement of high-order photoelectron emission, allowing for single-shot CEP and pulse duration

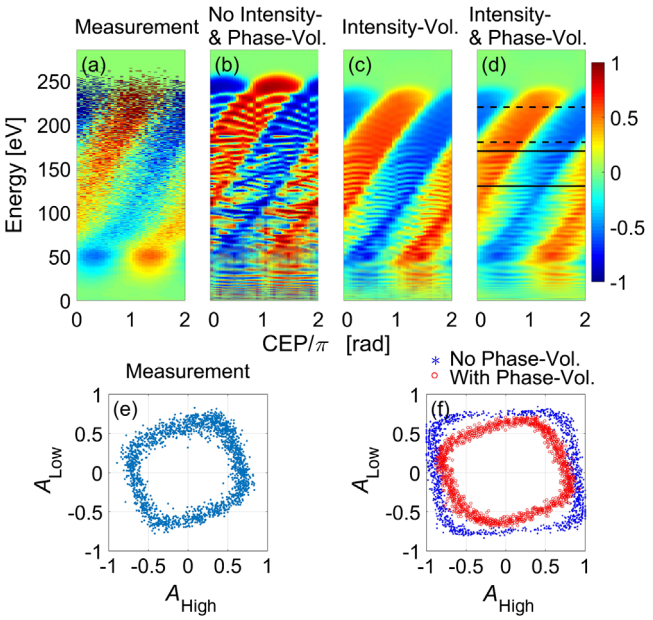

FIG. 2. Comparison between the measurements and the simulations of the strong-field ionization of xenon at 1800 nm. (a) Measured asymmetry with $\tau = 11.8 \pm 0.5$ fs, $I_0 = (0.8 \pm 0.2) \times 10^{14}$ W/cm^2. (b) Simulated asymmetry excluding the intensity- and phase- averaging effect with $\tau = 12$ fs, $I_0 = 0.8 \times 10^{14}$ W/cm^2. (c) Simulated asymmetry including only the intensity-volume effect. (d) Simulated asymmetry including both effects. (e) Measured PAP by a CEPM with 10.4 ± 0.5 fs pulses at 1800 nm. (f) Simulated PAPs with $\tau = 10$ fs pulses. The blue and red dots represent the case with and without the phase-volume effect, respectively. Two energy regions within black dashed lines and black solid lines in (d) are selected to obtain the PAPs.

measurement. The CEPM has been detailed in previous publications [40–42], thus only the salient points will be addressed here. In the CEPM, two detectors located on the left and right side along the laser polarization measure the high-order CEP-dependent photoelectron spectra for each single laser shot. In order to extract the CEP, two energy regions, i.e., one low and one high, are selected, [regions between the dashed lines and solid lines in Fig. 2(d)]. Integration of two spectra in each energy region yields four quantities, $Y_{\text{left-low}}$, $Y_{\text{left-high}}$, $Y_{\text{right-low}}$, and $Y_{\text{right-high}}$. By taking the normalized difference in each energy region, two sinusoidal-like CEP-dependent asymmetries are obtained,

$$A_{\text{low}} = \frac{Y_{\text{left-low}} - Y_{\text{right-low}}}{Y_{\text{left-low}} + Y_{\text{right-low}}} \approx A_0 \sin(\phi + \phi_0), \quad (4)$$

$$A_{\text{high}} = \frac{Y_{\text{left-high}} - Y_{\text{right-high}}}{Y_{\text{left-high}} + Y_{\text{right-high}}} \approx A_0 \sin(\phi + \phi_0 + \phi_i), \quad (5)$$

where A_0 is the asymmetry amplitude, ϕ is the CEP, ϕ_0 is an arbitrary but fixed offset phase and ϕ_i is the relative phase between two energy regions.

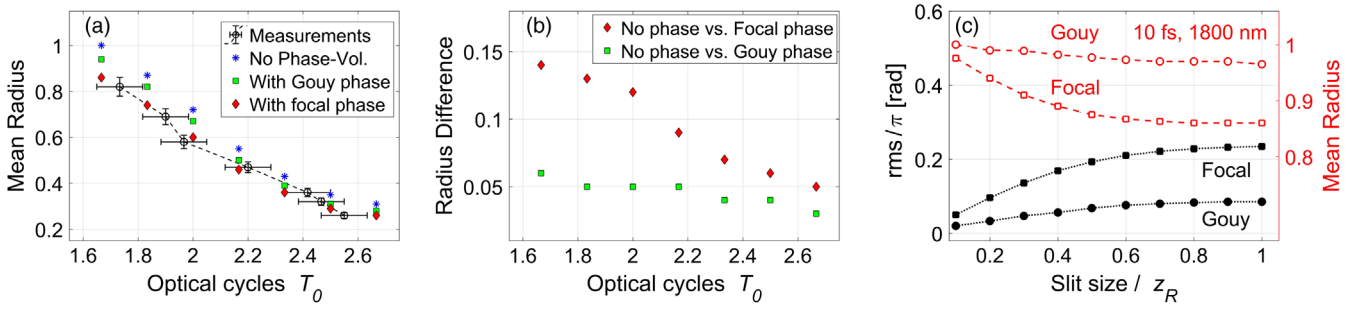

FIG. 3. (a) Comparison between pulse duration measurements with a CEPM and simulations at 1800 nm. The measurements are calibrated with a home-built frequency-resolved optical gating device. (b) Difference between no phase-volume effect included and including the Gouy phase or the focal phase. (c) rms of the phase distribution of strong-field ionization in xenon with different slit sizes and the corresponding PAP radii of 10-fs pulses at 1800 nm.

A so-called parametric asymmetry plot (PAP) is obtained by plotting two asymmetries, A_{high} and A_{low}, as x and y coordinates. One point in the PAP corresponds to one laser shot measurement and the polar angle in the PAP has a one-to-one correspondence to the CEP. As larger radius of the PAP implies a stronger CEP dependence, the PAPs serve as a simplified way to visualize the strength of the CEP dependence.

The measured PAPs by a CEPM with 10.4-fs pulses at 1800 nm are shown in Fig. 2(e). Accordingly, the simulated PAPs are presented in Fig. 2(f). The red dots (inner circle) and blue dots (outer circle) are the simulated intensity-averaged traces with and without the focal phase, respectively. Including the focal phase in the theoretical model reduces the radius of the PAP due to the averaging effect on the CEP and shows a good agreement with the measurement while those exclusions overestimate the radius—the CEP dependence.

As the significance of the CEP increases with a decrease in pulse length and direct high-accuracy measurements of few-cycle pulse length are exceedingly difficult, the strength of the CEP-dependence can also serve as a good way for pulse length calibration. However, not taking the phase distribution into account or not properly accounting for the focal phase may lead one to significantly overestimate the pulse duration. The pulse duration measurements of few-cycle pulses at 1800 nm with a CEPM are shown in Fig. 3(a). Unsurprisingly, the simulation excluding the focal phase always predicts larger radii than the measurements. Though the radii slightly shrink when the Gouy phase is taken into account in the simulation [green, square dots in Figs. 3(a) and 3(b)], large discrepancies still remain compared to the measurements. Apparently, the focal phase needs to be considered for a more realistic analysis. The radii of the PAPs further shrink when the focal phase is considered, which results in a better agreement with the measurements. This facilitates a better pulse duration calibration with a CEPM. In general, excluding the intensity- and phase-volume effect will lead one to expect a significantly larger phase dependence than is measured and inversely, these exclusions will lead one to believe that their pulse is longer and less intense than in reality.

In order to verify that these observations are not limited to a specific process or experimental parameters, we perform the measurement and simulations of strong-field ionization using few-cycle pulses at 750 nm additionally, see the Supplemental Material [37]. By shifting the wavelength and keeping the intensity, we change the regime of strong-field ionization between the tunnel ionization and multiphoton ionization, which can be distinguished by the Keldysh parameter [43]. Observing the same significant phase-volume effect at 750 nm as at 1800 nm, validates our theoretical treatment and predicts that this effect is not limited to some specific processes.

In order to reduce the phase-volume effect, the interaction volume in the experiments is often confined by inserting a small slit in the focus or using a beam target which behaves as an effective slit with respect to the Rayleigh range of the laser beam. In the simulation, we investigate how the size of the slit influence the phase-volume effect. The rms of the phase distribution with different sizes of the slit and the corresponding radius of the PAP from a 10-fs pulse at 1800 nm as an instance are shown in Fig. 3(c). With opening the size, the rms increases as more phase-volume effects are introduced. Thus, the radius of the PAP decreases. When the size of the slit is comparable to one Rayleigh range of the laser beam, the rms and the radius of the PAP maintain, because the yield at positions far away from the laser focus dramatically drops due to the low intensity. As long as the slit size is larger than z_R, it has no significant impact for reducing the phase effect. Even for slit sizes $> 0.5z_R$, the influence is small. If one wants to suppress the phase-volume effect efficiently, a beam or slit size $< 0.5z_R$ is desired. Note that the consequence of using a small slit is a reduction of the yield, e.g., ~30% less in strong-field ionization when the volume is confined to $0.5z_R$.

So far, we have discussed the phase-volume effect in strong-field ionization, which is a highly nonlinear physical process, for which the interaction volume is inherently

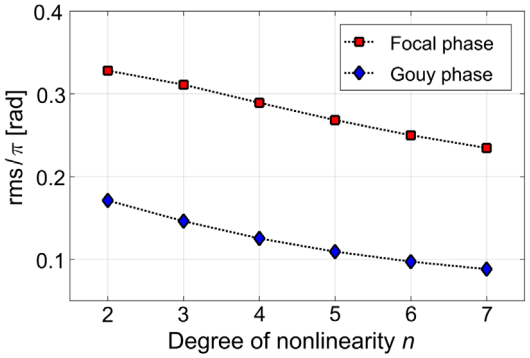

FIG. 4. rms of the phase distribution for light-matter interactions with different degrees of nonlinearity, n, with the probability of events, $P \sim I^n$, where I is the laser intensity.

confined by the strongly nonlinear intensity dependence of the yield. However, the phase-volume effect still cannot be neglected for such a highly nonlinear process and this situation is even worse for processes with lower nonlinearities, such as molecular dissociation [44], and multiphoton absorption [45] among others due to the larger effective interaction volume determined by the intensity-dependent yield. To address this issue and estimate the phase-volume effect for a broad range of few-cycle laser-induced dynamics, we introduce a parameter describing the probability of events P, as a function of the intensity, $P \sim I^n$, where I is the laser intensity and n can be considered as the degree of nonlinearity. Using this formulation we can determine how much the CEP dependence will be washed away for a given process. For example, the ADK ionization rate for xenon can be approximated as $n = 6$. Scanning over the nonlinear parameter, n, yields an n-dependent rms of the phase distribution, see Fig. 4. The larger rms indicates an even stronger phase-volume effects for lower-order nonlinear phenomena. This provides a quick and simple method for quantifying the phase-volume effect for a given process.

In conclusion, by comparing the measurements and the simulations of CEP-dependent photoelectron spectra of xenon, we quantify the phase-volume effect in strong-field ionization as a baseline and further expand the quantification of this effect to a broad range of few-cycle light-matter interactions with different degrees of nonlinearity. The theoretical analysis including the more realistic distribution of the focal phase shows a good agreement with the measurements, which allows us more accurate modeling and interpretation of the CEP-dependent few-cycle laser-induced processes. Conversely, the exclusions of the intensity- and phase-volume effect will predict longer, less intense pulses and larger CEP-dependence than actually measured in reality.

We acknowledge funding support from PA730/7 within Priority Program 1840, "Quantum Dynamics in Tailored Intense Fields" of the Deutsche Forschungsgemeinschaft (DFG).

*Corresponding author.
yinyu.zhang@uni-jena.de

[1] M. Chini, K. Zhao, and Z. Chang, The generation, characterization and applications of broadband isolated attosecond pulses, Nat. Photonics **8**, 178 (2014).
[2] F. Böhle, M. Kretschmar, A. Jullien, M. Kovacs, M. Miranda, R. Romero, H. Crespo, U. Morgner, P. Simon, R. Lopez-Martens *et al.*, Compression of CEP-stable multi-mJ laser pulses down to 4 fs in long hollow fibers, Laser Phys. Lett. **11**, 095401 (2014).
[3] V. Cardin, N. Thiré, S. Beaulieu, V. Wanie, F. Légaré, and B. E. Schmidt, 0.42 TW 2-cycle pulses at 1.8 μm via hollow-core fiber compression, Appl. Phys. Lett. **107**, 181101 (2015).
[4] G. Fan, T. Balčiūnas, T. Kanai, T. Flöry, G. Andriukaitis, B. E. Schmidt, F. Légaré, and A. Baltuška, Hollow-core-waveguide compression of multi-millijoule CEP-stable 3.2 μm pulses, Optica **3**, 1308 (2016).
[5] M. Gebhardt, C. Gaida, T. Heuermann, F. Stutzki, C. Jauregui, J. Antonio-Lopez, A. Schulzgen, R. Amezcua-Correa, J. Limpert, and A. Tünnermann, Nonlinear pulse compression to 43 W GW-class few-cycle pulses at 2 μm wavelength, Opt. Lett. **42**, 4179 (2017).
[6] U. Elu, M. Baudisch, H. Pires, F. Tani, M. H. Frosz, F. Köttig, A. Ermolov, P. S. J. Russell, and J. Biegert, High average power and single-cycle pulses from a mid-IR optical parametric chirped pulse amplifier, Optica **4**, 1024 (2017).
[7] H. Timmers, Y. Kobayashi, K. F. Chang, M. Reduzzi, D. M. Neumark, and S. R. Leone, Generating high-contrast, near single-cycle waveforms with third-order dispersion compensation, Opt. Lett. **42**, 811 (2017).
[8] R. Budriūnas, T. Stanislauskas, J. Adamonis, A. Aleknavičius, G. Veitas, D. Gadonas, S. Balickas, A. Michailovas, and A. Varanavičius, 53 W average power CEP-stabilized OPCPA system delivering 5.5 TW few cycle pulses at 1 kHz repetition rate, Opt. Exp. **25**, 5797 (2017).
[9] F. Silva, B. Alonso, W. Holgado, R. Romero, J. San Román, E. C. Jarque, H. Koop, V. Pervak, H. Crespo, and Í. J. Sola, Strategies for achieving intense single-cycle pulses with in-line post-compression setups, Opt. Lett. **43**, 337 (2018).
[10] F. Krausz and M. Ivanov, Attosecond physics, Rev. Mod. Phys. **81**, 163 (2009).
[11] F. Ferrari, F. Calegari, M. Lucchini, C. Vozzi, S. Stagira, G. Sansone, and M. Nisoli, High-energy isolated attosecond pulses generated by above-saturation few-cycle fields, Nat. Photonics **4**, 875 (2010).
[12] P. Heissler, R. Hörlein, J. M. Mikhailova, L. Waldecker, P. Tzallas, A. Buck, K. Schmid, C. M. S. Sears, F. Krausz, L. Veisz, M. Zepf, and G. D. Tsakiris, Few-Cycle Driven Relativistically Oscillating Plasma Mirrors: A Source of Intense Isolated Attosecond Pulses, Phys. Rev. Lett. **108**, 235003 (2012).
[13] N. Ishii, K. Kaneshima, K. Kitano, T. Kanai, S. Watanabe, and J. Itatani, Carrier-envelope phase-dependent high harmonic generation in the water window using few-cycle infrared pulses, Nat. Commun. **5**, 3331 (2014).
[14] O. Schubert, M. Hohenleutner, F. Langer, B. Urbanek, C. Lange, U. Huttner, D. Golde, T. Meier, M. Kira, S. W. Koch *et al.*, Sub-cycle control of terahertz high-harmonic

generation by dynamical Bloch oscillations, Nat. Photonics **8**, 119 (2014).
[15] S. Cousin, F. Silva, S. Teichmann, M. Hemmer, B. Buades, and J. Biegert, High-flux table-top soft x-ray source driven by sub-2-cycle, CEP stable, 1.85-μm 1-kHz pulses for carbon K-edge spectroscopy, Opt. Lett. **39**, 5383 (2014).
[16] Y. Bai, L. Song, R. Xu, C. Li, P. Liu, Z. Zeng, Z. Zhang, H. Lu, R. Li, and Z. Xu, Waveform-Controlled Terahertz Radiation from the Air Filament Produced by Few-Cycle Laser Pulses, Phys. Rev. Lett. **108**, 255004 (2012).
[17] T. Balčiūnas, D. Lorenc, M. Ivanov, O. Smirnova, A. Zheltikov, D. Dietze, K. Unterrainer, T. Rathje, G. Paulus, A. Baltuška *et al.*, CEP-stable tunable THz-emission originating from laser-waveform-controlled sub-cycle plasma-electron bursts, Opt. Express **23**, 15278 (2015).
[18] D. Milošević, G. Paulus, D. Bauer, and W. Becker, Above-threshold ionization by few-cycle pulses, J. Phys. B **39**, R203 (2006).
[19] N. G. Johnson, O. Herrwerth, A. Wirth, S. De, I. Ben-Itzhak, M. Lezius, B. Bergues, M. F. Kling, A. Senftleben, C. D. Schröter, R. Moshammer, J. Ullrich, K. J. Betsch, R. R. Jones, A. M. Sayler, T. Rathje, K. Rühle, W. Müller, and G. G. Paulus, Single-shot carrier-envelope-phase-tagged ion-momentum imaging of nonsequential double ionization of argon in intense 4-fs laser fields, Phys. Rev. A **83**, 013412 (2011).
[20] M. Kübel, C. Burger, N. G. Kling, T. Pischke, L. Beaufore, I. Ben-Itzhak, G. G. Paulus, J. Ullrich, T. Pfeifer, R. Moshammer *et al.*, Complete characterization of single-cycle double ionization of argon from the nonsequential to the sequential ionization regime, Phys. Rev. A **93**, 053422 (2016).
[21] W. Becker, S. Goreslavski, D. Milošević, and G. Paulus, The plateau in above-threshold ionization: The keystone of rescattering physics, J. Phys. B **51**, 162002 (2018).
[22] T. Rathje, A. M. Sayler, S. Zeng, P. Wustelt, H. Figger, B. D. Esry, and G. G. Paulus, Coherent Control at its Most Fundamental: Carrier-Envelope-Phase-Dependent Electron Localization in Photodissociation of a H_2^+ Molecular Ion Beam Target, Phys. Rev. Lett. **111**, 093002 (2013).
[23] X. M. Tong and C. D. Lin, Dynamics of Light-Field Control of Molecular Dissociation at the Few-Cycle Limit, Phys. Rev. Lett. **98**, 123002 (2007).
[24] H. Li *et al.*, Coherent Electronic Wave Packet Motion in C_{60} Controlled by the Waveform and Polarization of Few-Cycle Laser Fields, Phys. Rev. Lett. **114**, 123004 (2015).
[25] N. G. Kling, K. J. Betsch, M. Zohrabi, S. Zeng, F. Anis, U. Ablikim, B. Jochim, Z. Wang, M. Kübel, M. F. Kling, K. D. Carnes, B. D. Esry, and I. Ben-Itzhak, Carrier-Envelope Phase Control Over Pathway Interference in Strong-Field Dissociation of H_2^+, Phys. Rev. Lett. **111**, 163004 (2013).
[26] S. Y. Kruchinin, F. Krausz, and V. S. Yakovlev, Colloquium: Strong-field phenomena in periodic systems, Rev. Mod. Phys. **90**, 021002 (2018).
[27] L. G. Gouy, *Sur Une Propriété Nouvelle Des Ondes Lumineuses* (Gauthier-Villars, Paris, 1890).
[28] A. Sayler, P. Wang, K. Carnes, and I. Ben-Itzhak, Determining intensity dependence of ultrashort laser processes through focus z-scanning intensity-difference spectra: application to laser-induced dissociation of H_2^+, J. Phys. B **40**, 4367 (2007).
[29] M. Ammosov, N. Delone, V. Krainov, A. Perelomov, V. Popov, M. Terentev, G. L. Yudin, and M. Y. Ivanov, Tunnel ionization of complex atoms and of atomic ions in an alternating electromagnetic field, Sov. Phys. JETP **64**, 26 (1986), http://www.jetp.ac.ru/cgi-bin/e/index/e/64/6/p1191?a=list.
[30] F. Lindner, G. G. Paulus, H. Walther, A. Baltuška, E. Goulielmakis, M. Lezius, and F. Krausz, Gouy Phase Shift for Few-Cycle Laser Pulses, Phys. Rev. Lett. **92**, 113001 (2004).
[31] T. Tritschler, K. Hof, M. Klein, and M. Wegener, Variation of the carrier-envelope phase of few-cycle laser pulses owing to the Gouy phase: a solid-state-based measurement, Opt. Lett. **30**, 753 (2005).
[32] Q. Lin, J. Zheng, and W. Becker, Subcycle Pulsed Focused Vector Beams, Phys. Rev. Lett. **97**, 253902 (2006).
[33] M. A. Porras, Diffraction effects in few-cycle optical pulses, Phys. Rev. E **65**, 026606 (2002).
[34] M. A. Porras, Characterization of the electric field of focused pulsed Gaussian beams for phase-sensitive interactions with matter, Opt. Lett. **34**, 1546 (2009).
[35] M. A. Porras, Z. L. Horváth, and B. Major, Three-dimensional carrier-envelope-phase map of focused few-cycle pulsed Gaussian beams, Phys. Rev. A **98**, 063819 (2018).
[36] D. Hoff, M. Krüger, L. Maisenbacher, A. M. Sayler, G. G. Paulus, and P. Hommelhoff, Tracing the phase of focused broadband laser pulses, Nat. Phys. **13**, 947 (2017).
[37] See the Supplemental Material at http://link.aps.org/supplemental/10.1103/PhysRevLett.124.133202 for the description of the intensity- and phase-dependent yield and strong-field ionization of xenon using few-cycle pulses at 750 nm.
[38] P. Agostini, F. Fabre, G. Mainfray, G. Petite, and N. K. Rahman, Free-Free Transitions Following Six-Photon Ionization of Xenon Atoms, Phys. Rev. Lett. **42**, 1127 (1979).
[39] W. Becker, F. Grasbon, R. Kopold, D. Milosevic, G. Paulus, and H. Walther, Above-threshold ionization: From classical features to quantum effects, Adv. At. Mol. Opt. Phys. **48**, 35 (2002).
[40] A. Sayler, T. Rathje, W. Müller, C. Kürbis, K. Rühle, G. Stibenz, and G. Paulus, Real-time pulse length measurement of few-cycle laser pulses using above-threshold ionization, Opt. Express **19**, 4464 (2011).
[41] A. Sayler, T. Rathje, W. Müller, K. Rühle, R. Kienberger, and G. Paulus, Precise, real-time, every-single-shot, carrier-envelope phase measurement of ultrashort laser pulses, Opt. Lett. **36**, 1 (2011).
[42] Y. Zhang, P. Kellner, D. Adolph, D. Zille, P. Wustelt, D. Würzler, S. Skruszewicz, M. Möller, A. M. Sayler, and G. G. Paulus, Single-shot, real-time carrier-envelope phase measurement and tagging based on stereographic above-threshold ionization at short-wave infrared wavelengths, Opt. Lett. **42**, 5150 (2017).
[43] L. Keldysh *et al.*, Ionization in the field of a strong electromagnetic wave, Sov. Phys. JETP **20**, 1307 (1965), http://www.jetp.ac.ru/cgi-bin/e/index/e/20/5/p1307?a=list.
[44] G. Jolicard and O. Atabek, Above-threshold-dissociation dynamics of H_2^+ with short intense laser pulses, Phys. Rev. A **46**, 5845 (1992).
[45] G. Agarwal, Field-correlation effects in multiphoton absorption processes, Phys. Rev. A **1**, 1445 (1970).